viral responder, regardless of the fact that successful immune responses have been induced in a substantial number of patients. The well-recognized difficulty of developing either prophylactic or therapeutic HCV vaccines largely results from viral heterogeneity and mutability (6-8). In addition, many studies have demonstrated suppressed or imbalanced immunity in CH or LC patients with HCV (25,26,30). Previous and present results, when taken together, suggest that developing an HCV vaccine to induce SVR as a primary endpoint will not be feasible until novel scientific breakthroughs in this field have been made. However, HCV peptide vaccines may augment both cellular and humoral responses against HCV-derived peptides in a large percentage of patients. This potential of peptide vaccines provides some hope that boosted specific immunity eliminates cancerous liver cells infected with HCV, which in turn may result in prevention or delay of HCC development associated with HCV. Indeed, the results of the present study support this hypothesis. Further clinical studies are required to confirm whether or not peptide vaccination using CTL epitopes derived from HCV protein are effective for prophylaxis against HCC in HCV-positive patients without SOL.

Acknowledgements

This study was supported in part by Grants-in-Aid from the Ministry of Education, Science, Sports and Culture of Japan to the Research Center of Innovative Cancer Therapy of the 21st Century Center of Excellence (COE) Program for Medical Science, and to Toshi-area Research.

References

1. World Health Organization (WHO) Hepatitis C. 2006. Available at: http://www.who.int/vaccine_research/diseases/viral_cancers/en/index2.html#disease%20burden
2. Chander G, Sulkowski MS, Jenckes MW, Torbenson MS, Herlong HF, Bass EB and Gebo KA: Treatment of chronic hepatitis C: a systematic review. Hepatology 36: S135-S144, 2002.
3. Kato N, Hijikata M, Ootsuyama Y, Nakagawa M, Ohkoshi S and Sugimura T: Molecular cloning of the human hepatitis C virus genome from Japanese patients with non-A, non-B hepatitis. Proc Natl Acad Sci USA 87: 9524-9528, 1990.
4. Blatt LM, Mutchnick MG, Tong MJ, *et al*: Assessment of hepatitis C virus RNA and genotype from 6807 patients with chronic hepatitis C in the United States. J Viral Hepat 7: 196-202, 2000.
5. Yoshida H, Shiratori Y, Moriyama M, *et al*: Interferon therapy reduces the risk for hepatocellular carcinoma: national surveillance program of cirrhotic and noncirrhotic patients with chronic hepatitis C in Japan. IHIT Study Group. Inhibition of Hepatocarcinogenesis by Interferon Therapy. Ann Intern Med 131: 174-181, 1999.
6. Houghton M and Abrignani S: Prospects for a vaccine against the hepatitis C virus. Nature 436: 961-966, 2005.
7. Strickland GT, El-Kamary SS, Klenerman P and Nicosia A: Hepatitis C vaccine: supply and demand. Lancet Infect Dis 8: 379-386, 2008.
8. Bowen DG and Walker CM: Mutational escape from CD8+ T cell immunity: HCV evolution, from chimpanzees to man. J Exp Med 201: 1709-1714, 2005.
9. Schlaphoff V, Klade CS, Jilma B, *et al*: Functional and phenotypic characterization of peptide-vaccine-induced HCV-specific CD8+ T cells in healthy individuals and chronic hepatitis C patients. Vaccine 25: 6793-6806, 2007.
10. Klade CS, Wedemeyer H, Berg T, *et al*: Therapeutic vaccination of chronic hepatitis C nonresponder patients with the peptide vaccine IC41. Gastroenterology 134: 1385-1395, 2008.
11. Yutani S, Yamada A, Yoshida K, *et al*: Phase I clinical study of a personalized peptide vaccination for patients infected with hepatitis C virus (HCV) 1b who failed to respond to interferon-based therapy. Vaccine 25: 7429-7435, 2007.
12. Yutani S, Komatsu N, Shichijo S, *et al*: Phase I clinical study of a peptide vaccination for hepatitis C virus-infected patients with different HLA-class I-A alleles. Cancer Science 100: 1935-1942, 2009.
13. Leroux-Roels G, Batens AH, Desombere I, *et al*: Immunogenicity and tolerability of intradermal administration of an HCV E1-based vaccine candidate in healthy volunteers and patients with resolved or ongoing chronic HCV infection. Hum Vaccin 1: 61-65, 2005.
14. Niu Y, Terasaki Y, Komatsu N, *et al*: Identification of peptides applicable as vaccines for HLA-A26-positive cancer patients. Cancer Science 100: 2167-2174, 2009.
15. Cerny A, McHutchison JG, Pasquinelli C, *et al*: Cytotoxic T lymphocyte response to hepatitis C virus-derived peptides containing the HLA A2.1 binding motif. J Clin Invest 95: 521-530, 1995.
16. Kiyosawa K, Umemura T, Ichijo T, *et al*: Hepatocellular carcinoma: recent trends in Japan. Gastroenterology 127: S17-S26, 2004.
17. Taura K, Ikai I, Hatano E, *et al*: Influence of coexisting cirrhosis on outcomes after partial hepatic resection for hepatocellular carcinoma fulfilling the Milan criteria: an analysis of 293 patients. Surgery 142: 685-694, 2007.
18. Shiratori Y, Shiina S, Teratani T, *et al*: Interferon therapy after tumor ablation improves prognosis in patients with hepatocellular carcinoma associated with hepatitis C virus. Ann Intern Med 138: 299-306, 2003.
19. Kubo M, Sakaguchi Y, Chung H, *et al*: Long-term interferon maintenance therapy improves survival in patients with HCV-related hepatocellular carcinoma after curative radiofrequency ablation. A matched case-control study. Oncology 72: 132-138, 2007.
20. Kim JH, Han KH, Lee KS, *et al*: Efficacy and long term follow up of combination therapy with interferon alpha and ribavirin for chronic hepatitis C in Korea. Yonsei Medical Journal 47: 793-798, 2006.
21. Arase Y, Ikeda K, Suzuki F, *et al*: Long term outcome after interferon therapy in elderly patients with chronic hepatitis C. Intervirology 50: 16-23, 2007.
22. Ikeda K, Saitoh S, Arase Y, *et al*: Effect of interferon therapy on hepatocellular carcinogenesis in patients with chronic hepatitis type C: a long-term observation study of 1,643 patients using statistical bias correction with proportional hazard analysis. Hepatology 29: 1124-1130, 1999.
23. Toyoda H, Kumada T, Tokuda A, *et al*: Long-term follow-up of sustained responders to interferon therapy in patients with chronic hepatitis C. J Viral Hepatitis 7: 414-419, 2007.
24. Okanoue T, Itoh Y, Minami M, *et al*: Interferon therapy lowers the rate of progression to hepatocellular carcinoma in chronic hepatitis C but not significantly in an advanced stage: a retrospective study in 1148 patients. J Hepatol 30: 643-649, 1999.
25. Bertoketti A, Bertoletti A, D'Elios MM, *et al*: Different cytokine profiles of intrahepatic T cells in chronic hepatitis B and hepatitis C virus infections. Gastroenterology 112: 193-199, 1997.
26. McGuinness PH, Painter D, Davies S and McCaughan GW: Increases in intrahepatic CD68 positive cells, MAC387 positive cells and proinflammatory cytokines (particularly interleukin 18) in chronic hepatitis C infection. Gut 46: 260-269, 2000.
27. Nelson DR, Lauwers GY, Lau JY and Davis GL: Interleukin 10 treatment reduces fibrosis in patients with chronic hepatitis C: a pilot trial of interferon nonresponders. Gastroenterology 118: 655-660, 2000.
28. Brière F, Servet-Delprat C, Bridon JM, Saint-Remy JM and Banchereau J: Human interleukin 10 induces naive surface immunoglobulin D+ (sIgD+) B cells to secrete IgG1 and IgG3. J Exp Med 179: 757-762, 1994.
29. Defrance T, Vanbervliet B, Brière F, *et al*: Interleukin 10 and transforming growth factor beta cooperate to induce anti-CD40-activated naive human B cells to secrete immunoglobulin A. J Exp Med 175: 671-682, 1992.
30. Rushbrook SM, Ward SM, Unitt E, *et al*: Regulatory T cells suppress in vitro proliferation of virus-specific CD8+ T cells during persistent hepatitis C virus infection. J Virol 79: 7852-7859, 2005.

Table 1 Selected differential disgnosis of fibrosing alopecia in a pattern distribution

Condition	Characteristics	Histology
Fibrosing alopecia in a pattern distribution	Alopecia in the distribution of typical male or female pattern hair loss Perifollicular erythema and hyperkeratosis	Miniaturization of hair follicles Lichenoid inflammatory infiltrate at isthmus and infundibular region perifollicular lamellar fibrosis
Androgenetic alopecia	Pattern baldness on the bitemporal areas and crown of the scalp	Miniaturized vellus follicles Increased telogen hairs in late stage
Frontal fibrosing alopecia	Cicatricial frontotemporal hair line recession Almost exclusively in postmenopausal women Perifollicular erythema and hyperkeratosis	Perifollicular fibrosis Lymphocytic infiltration at the isthmus and infundibulum
Follicular degeneration syndrome	Cicatricial alopecia of the central scalp and enlarges centrifugally	Premature inner root sheath desquamation Lymphocytic infiltration at the upper follicle Perifollicular concentric fibrosis
Pseudopelade of Brocq	Multiple round or irregularly shaped, hairless, cicatrial patches	Early stage: perifollicular lymphocytic infiltration Late stage: follicular longitudinal fibrous tract extended into subcutis

replacement of follicles with fibrosis in cicatricial alopecia. The striking differences between AGA/FPHL and FAPD include perifollicular erythema, perifollicular hyperkeratosis and loss of follicular orifices in the central scalp in FAPD.[1,3]

Cicatricial alopecia, including frontal fibrosing alopecia (FFP), follicular degeneration syndrome (FDS) and pseudopelade of Brocq share some clinical and histological evidence of the scarring process with FAPD.[1]

Frontal fibrosing alopecia is characterized with unique cicatricial frontotemporal hair line recession and almost exclusively presents in postmenopausal women.[5] Centrifugal and progressive hair loss starting at midscalp in our patient make the diagnosis of FFP less likely. Unlike FAPD, miniaturized hair follicles are rarely observed in FFP.

Pseudopelade of Brocq usually presents with multiple round, oval or irregularly shaped, hairless, cicatrial patches of varying sizes, which can distinguish it from FAPD.[5] Follicular erythema and hyperkeratosis are not typical features in pseudopelade of Brocq.

Follicular degeneration syndrome is a condition that presents with flesh-coloured, non-inflammatory cicatricial alopecia of the central scalp that, over time, enlarges centrifugally.[5] Histologically, the premature degeneration of the inner root sheath and migration of the hair shaft through the outer root sheath in the follicular degeneration are not seen in the histology of FAPD.[1,4]

Author contributions

Hsien-Yi Chiu: drafting of the manuscript, Sung-Jan Lin: case management and critical revision of the manuscript.

H-Y Chiu,[†] S-J Lin[†,‡,*]

[†]Department of Dermatology, National Taiwan University Hospital and National Taiwan University College of Medicine, Taipei, Taiwan, and [‡]Institute of Biomedical Engineering, National Taiwan University, Taipei, Taiwan

*Correspondence: S-J Lin. E-mail: drsjlin@ntu.edu.tw

References

1 Zinkernagel MS, Trueb RM. Fibrosing alopecia in a pattern distribution: patterned lichen planopilaris or androgenetic alopecia with a lichenoid tissue reaction pattern? *Arch Dermatol* 2000; **136**: 205–211.
2 Kossard S. Postmenopausal frontal fibrosing alopecia. Scarring alopecia in a pattern distribution. *Arch Dermatol* 1994; **130**: 770–774.
3 Olsen EA. Female pattern hair loss and its relationship to permanent/cicatricial alopecia: a new perspective. *J Investig Dermatol Symp Proc* 2005; **10**: 217–221.
4 Sperling LC, Solomon AR, Whiting DA. A new look at scarring alopecia. *Arch Dermatol* 2000; **136**: 235–242.
5 Ross EK, Tan E, Shapiro J. Update on primary cicatricial alopecias. *J Am Acad Dermatol* 2005; **53**: 1–37; quiz 8–40.

DOI: 10.1111/j.1468-3083.2010.03580.x

Questionnaire-based survey of the treatment of patients with psoriasis and hepatitis C in Japan

Editor

Hepatitis C virus (HCV) is the most frequent aetiology of hepatitis in Japan, and a total of 1.5–2 million (1.2–1.5%) of Japanese are considered to be HCV positive. Combination therapy with pegylated interferon (IFN) alpha and ribavirin can eradicate approximately 80% of the HCV in chronic hepatitis C patients.[1] However, this therapy has various side-effects including the induction and/or exacerbation of psoriasis and psoriatic arthritis.[2–4] Therefore, HCV-positive patients with psoriasis encounter serious problems during treatment for their hepatitis.

Such patients also have problems in treating their psoriasis. Cyclosporine A (CyA), the most useful oral medication available

© 2010 The Authors
Journal compilation © 2010 European Academy of Dermatology and Venereology

for psoriasis in Japan, was contraindicated for patients with chronic infections because of its strong immunosuppressive potential. However, recent research has revealed that CyA suppresses HCV replication *in vitro*[5,6] and *in vivo*.[7] We also previously reported a case of patients with psoriasis and hepatitis C successfully treated with CyA without worsening of their hepatitis.[8] To reach a consensus in treating HCV-positive patients with psoriasis, it is important to understand the current situation of the treatment modalities for such patients. Therefore, we carried out a questionnaire-based survey to estimate the frequency of HCV-positive patients with psoriasis in Japan and how they are treated.

A questionnaire asking the number of the patients with psoriasis and hepatitis C, and the dermatological and hepatological therapies was sent to dermatologists who were all members of the Japanese Dermatological Association (JDA).

A total of 234 completed questionnaires (38.9%) were returned (Table 1). Overall, 38% (88/234) of the dermatologists were treating HCV-positive patients with psoriasis.

The dermatologists in the university hospitals treated HCV-positive psoriasis patients more frequently (52%, 61/118) than the dermatologists in community hospitals (30%, 17/56) and practitioners (18%, 11/60). On average, the dermatologists treated 1.25 HCV-positive psoriasis patients at university hospitals, 0.46 patients at community hospitals and 0.44 patients at clinics (overall average of 0.85 patients per dermatologist).

Dermatologists employed topical corticosteroid and topical vitamin D3 cream most frequently followed by phototherapy, and CyA was used by 24% of dermatologists (Fig. 1a).

On treating hepatitis C, glycyrrhizin or ursodeoxycholic acid was administered by 45% of the internists, while IFN alpha was chosen by 40% of the internists and maximum of 99 patients underwent IFN therapy. In 28% of the patients, the dermatologists were not aware of the hepatitis therapy their patients were undergoing (Fig. 1b).

Our results showed that 38% of dermatologists in Japan treated HCV-positive patients with psoriasis, providing an average of 0.85 such patients per dermatologist. Based on the total number of dermatologists in Japan, approximately 7000 HCV-positive psoriasis patients may reside in Japan. Dermatologists in HCV-thriving countries should be aware of how their patients are treated by internists.

In addition to topical therapies, 24% of the dermatologists used CyA to treat psoriasis in patients with hepatitis C. This finding reveals that dermatologists no longer consider CyA to be a contraindication for patients with hepatitis C. CyA is providing more preferable therapeutic results in HCV-positive recipients in liver

Table 1 Results for the returned questionnaires

Facilities	Sent	Returned	Return ratio (%)	No. dermatologists with a positive response	Positive ratio (%)	No. patients	Mean patient number per dermatologist
University hospitals	309	118	38.2	61	51.7	147	1.25
Community hospitals	128	56	43.8	17	30.4	30	0.54
Dermatology clinics	159	60	37.7	11	18.3	26	0.43
Total	596	234	39.3	89	38.0	198	0.85

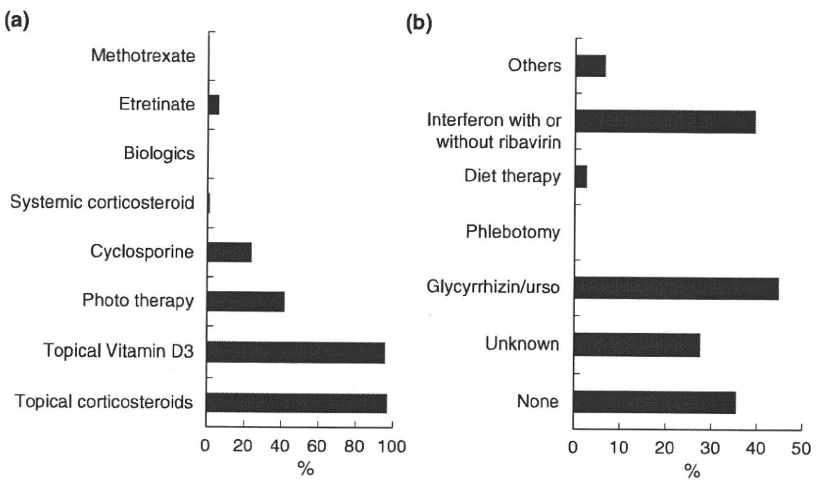

Figure 1 Treatment choices of (a) dermatologists and (b) internists for the treatment of patients with psoriasis and hepatitis C. Urso, ursodeoxycholic acid.

© 2010 The Authors
Journal compilation © 2010 European Academy of Dermatology and Venereology

transplantation[9] and HCV-positive patients with autoimmune diseases.[10]

Regarding the treatments for hepatitis employed by internists, it was a surprising finding that 40% of institutions employed IFN alpha therapy for patients with psoriasis. We plan to further examine the detailed information for these patients.

Twenty-eight per cent of dermatologists answered that they were not aware of the hepatitis therapies employed by the internists. As administration of IFN alpha has a risk of exacerbating psoriasis, dermatologists should know the way in which their patients are being treated by internists, and informed consent should be obtained from the patients before IFN alpha treatment.

Acknowledgements

This study was supported in part by Health and Labour Sciences Research Grants for Research on Hepatitis from the Ministry of Health, Labour and Welfare of Japan.

S Imafuku,* J Nakayama

Department of Dermatology, Faculty of Medicine, Fukuoka University, Fukuoka, Japan

*Correspondence: S Imafuku. E-mail: dermatologist@mac.com

References

1 Ide T, Hino T, Ogata K *et al.* A randomized study of extended treatment with peginterferon alpha-2b plus ribavirin based on time to HCV RNA negative-status in patients with genotype 1b chronic hepatitis C. *Am J Gastroenterol* 2009; **104**: 70–75.
2 Quesada JR, Gutterman JU. Psoriasis and alpha-interferon. *Lancet* 1986; **1**: 1466–1468.
3 Jucgla A, Marcoval J, Curco N, Servitje O. Psoriasis with articular involvement induced by interferon alfa. *Arch Dermatol* 1991; **127**: 910–911.
4 Gota C, Calabrese L. Induction of clinical autoimmune disease by therapeutic interferon-alpha. *Autoimmunity* 2003; **36**: 511–518.
5 Watashi K, Hijikata M, Hosaka M *et al.* Cyclosporin A suppresses replication of hepatitis C virus genome in cultured hepatocytes. *Hepatology* 2003; **38**: 1282–1288.
6 Watashi K, Ishii N, Hijikata M *et al.* Cyclophilin B is a functional regulator of hepatitis C virus RNA polymerase. *Mol Cell* 2005; **19**: 111–122.
7 Inoue K, Sekiyama K, Yamada M *et al.* Combined interferon alpha2b and cyclosporin A in the treatment of chronic hepatitis C: controlled trial. *J Gastroenterol* 2003; **38**: 567–572.
8 Imafuku S, Tashiro A, Furue M. Ciclosporin treatment of psoriasis in a patient with chronic hepatitis C. *Br J Dermatol* 2007; **156**: 1367–1369.
9 Cescon M, Grazi GL, Cucchetti A *et al.* Predictors of sustained virological response after antiviral treatment for hepatitis C recurrence following liver transplantation. *Liver Transpl* 2009; **15**: 782–789.
10 Manna R, Verrecchia E, Fonnesu C *et al.* Cyclosporine A: good response for patients affected by autoimmune disorders and HCV infection? *Eur Rev Med Pharmacol Sci* 2009; **1**: 63–69.

DOI: 10.1111/j.1468-3083.2010.03586.x

A missense mutation in KRT14 causing a dermatopathia pigmentosa reticularis/Naegeli–Franceschetti–Jadassohn phenotype

Editor

Naegeli–Franceschetti–Jadassohn syndrome and dermatopathia pigmentosa reticularis (NFJS/DPR) are highly similar disorders characterized by core symptoms of reticular hyperpigmentation of the skin, palmoplantar keratoderma, nail dystrophy and reduced sweating. Various associated abnormalities include blistering, poor teeth, reduced or absent dermatoglyphics and hypotrichosis. In 2006, Lugassy *et al.* found heterozygous non-sense and frameshift mutations in the E1 and V1 domains of keratin 14 (KRT14) in five families with DPR/NFJS;[1] as a consequence, the two disorders are now considered allelic. All mutations were predicted to result in early termination of translation and it was speculated that KRT14 plays a role in early development of the epidermis and its appendages. The N-terminus has been shown to confer protection against apoptosis and increased apoptotic activity was indeed shown in the basal layer of patient epidermis.[2] The origin of the hyperpigmentation is less clear, but might relate to melanosome trafficking. Alternatively, pigmentary incontinence secondary to basal keratinocyte apoptosis might be responsible. Lugassy *et al.* have speculated that the NFJS/DPR mutations do not result in non-sense-mediated mRNA decay, but do allow for the production of a truncated KRT14 protein which then exerts a dominant negative effect. In support of their hypothesis, autosomal recessive EBS can be caused by truncating mutations affecting more distal domains of the protein.[3] However, formal proof for this hypothesis is lacking and finding a NFJS/DPR phenotype associated with more distal or missense mutations would put it in doubt. Here, we describe a patient with a DPR/NFJS phenotype caused by a missense mutation in KRT14.

The patient is a 41-year-old woman of Dutch descent who was referred to our outpatient clinic for flexural hyperpigmentation that had been present for as long as she could recall, but had been more pronounced when she was younger. She had never experienced blistering and did not complain of reduced sweating. Her nails did not grow well, but broke easily. The patient was otherwise healthy. There were no affected family members and she had no children. Upon physical examination, there was reticulate hyperpigmentation in both axillae, the neck and bilaterally in the inguinal region (Fig. 1a). Some mottled pigmentation was also visible on the dorsa of the fingers. The fingertips had reduced dermatoglyphics and there was clear nail dystrophy (Fig. 1b,c). Hair and teeth were normal. Blistering was absent. Based on the nail dystrophy, reduced dermatoglyphics and reticulate

© 2010 The Authors
Journal compilation © 2010 European Academy of Dermatology and Venereology

Chronic Hepatitis and Cirrhosis on MR Imaging

Tatsuyuki Tonan, MD[a], Kiminori Fujimoto, MD, PhD[a,b], Aliya Qayyum, MD, MRCP, FRCR[c,*]

KEYWORDS

- Liver cirrhosis • Hepatitis
- Liver-specific MR contrast agent • Fibrosis
- Regenerative nodule • Dysplastic nodule
- Well-differentiated hepatocellular carcinoma

Chronic liver diseases represent a major cause of morbidity and mortality worldwide. The major origins of chronic liver disease and also leading causes of cirrhosis and hepatocellular carcinoma (HCC) are chronic infection with hepatitis B virus (HBV) and hepatitis C virus (HCV), and alcoholic and nonalcoholic fatty liver disease. Magnetic resonance (MR) imaging has been increasingly used to evaluate diffuse parenchymal abnormalities of the liver. Morphologic changes and signal intensity effects not only facilitate the diagnosis of chronic liver disease with MR imaging, but may help to distinguish between differing etiology and assist in staging severity. Moreover, recent advances in the development of MR systems and liver-specific MR contrast agents such as superparamagnetic iron oxide (SPIO) and gadoxetic acid (Gd-EOB-DTPA) have expanded the potential utility of MR imaging in the accurate depiction of specific disorders and cirrhosis-associated hepatocellular nodules.

In this article, the authors focus on the current role of MR imaging in the detection and characterization of chronic hepatitis and cirrhosis. In particular, the characteristic MR imaging features of morphologic changes and focal manifestations of chronic liver disease are highlighted.

DEFINITION, ETIOLOGY, AND PREVALENCE

Chronic hepatitis is defined as a continuous or recurrent inflammation of the liver for more than 6 months, with histologic changes of chronic liver damage. Pathologically it is characterized by lymphocytic infiltration, liver cell injury, necrosis, and fibrosis.[1] Chronic hepatitis progresses from mild inflammation, to more severe inflammation and fibrosis, and eventually to cirrhosis. Cirrhosis is characterized by the replacement of liver tissue by fibrosis, scar tissue, and regenerative nodules, leading to the deterioration of liver function.[2]

The most common causes of cirrhosis in the United States[3] are HBV and HCV infection, either singly or combined, and alcohol abuse. Other causes of cirrhosis include nonalcoholic fatty liver disease, hemochromatosis, autoimmune disease, Wilson disease, primary sclerosing cholangitis, and primary biliary cirrhosis.

The clinical importance of chronic liver disease is reflected in the large numbers of affected patients and the frequency of the associated serious complications. Approximately 400 million people are chronically infected with HBV worldwide,[4] of whom 25% to 40% die of cirrhosis and its end-stage complications. Chronic hepatitis C further affects approximately 200 million people

[a] Department of Radiology, Kurume University School of Medicine, 67 Asahi-machi, Kurume 830-0011, Japan
[b] Department of Radiology, Center for Diagnostic Imaging, Kurume University Hospital, 67 Asahi-machi, Kurume 830-0011, Japan
[c] Department of Radiology and Biomedical Imaging, University of California San Francisco, 505 Parnassus Avenue, Room L-307, Box 0628, San Francisco, CA 94143, USA
* Corresponding author.
E-mail address: aliya.qayyum@radiology.ucsf.edu

Magn Reson Imaging Clin N Am 18 (2010) 383–402
doi:10.1016/j.mric.2010.08.011
1064-9689/10/$ – see front matter © 2010 Elsevier Inc. All rights reserved.

mri.theclinics.com

with a greater prevalence in Western countries.[5] The development of cirrhosis is common in chronic HCV, and the risk of HCC is 3% to 4% per year.[6] Once chronic HCV infection is established, cirrhosis develops within 10 to 20 years in approximately 20% of patients.[7] An estimated 10,000 deaths annually have been attributed to HCV-related diseases, and it is suggested that HCV may be responsible for nearly half of all HCC cases.

Alcoholic liver disease is among the most important causes of morbidity and mortality in the United States, accounting for up to 12,000 deaths each year, and representing more than 50% of liver disease–related deaths.[8,9] Nonalcoholic fatty liver disease (NAFLD) is now recognized as an important clinical entity, affecting approximately 20% to 30% of the adult population in the Western world.[10] NAFLD represents a disease spectrum ranging from isolated steatosis to more advanced disease with necroinflammatory change and fibrosis (nonalcoholic steatohepatitis or NASH), to cirrhosis in its most severe form. The prevalence of obesity and NAFLD in the United States translates into a substantial clinical problem, with more than 19% of obese individuals and 2% to 3% of the general population presenting with NASH.[10]

MR IMAGING FEATURES

Morphologic and Signal Intensity Changes

Hepatitis is associated with infiltration of inflammatory cells in to the liver, which results in liver cell injury and edema. Such liver changes may be visualized as periportal edema, which is characterized by high signal intensity bands paralleling the portal vessels on T2-weighted images (**Fig. 1**).

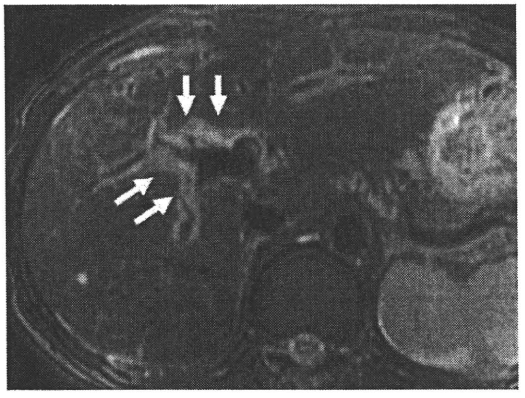

Fig. 1. T2-weighted fat-saturated turbo spin-echo (TSE) image (repetition time/echo time [TR/TE] = 4600/99 ms) in a patient with chronic hepatitis due to autoimmune hepatitis shows regions of high signal intensity bands paralleling the portal vessels (*arrow*).

Periportal edema is a common but nonspecific imaging finding in patients with severe acute hepatitis[11] and is also described in chronic viral hepatitis.[1] A similar appearance may also be seen in patients with malignant lymphadenopathy in the porta hepatis, biliary obstruction, cirrhosis, hepatic trauma, or transplant rejection.[12]

As cirrhosis progresses from early to advanced or end stage, it gives rise to several intra- and extrahepatic changes, including regional morphologic changes in the liver, nodularity of the liver surface, splenomegaly, regenerative nodules, iron and fat deposition, and ascites, and the development of varices and collaterals.[13] Although the classically described findings of cirrhosis are common in advanced cirrhosis, they are seen less frequently in the early stage of the disease, at which time the liver may appear normal on cross-sectional imaging, occasionally hampering imaging-based diagnosis.[14]

Enlargement of the hilar periportal space[14] (**Fig. 2**) on MR imaging has been shown to be a useful sign in the diagnosis of early cirrhosis. It has been reported that this sign is visible in 98% of patients with early cirrhosis who do not have conventional signs (ie, splenomegaly, portosystemic collateral vessels, ascites, or surface nodularity), whereas this sign is seen in only 11% of patients with normal livers.[15] Often, expansion of the major interlobar fissure[16] (see **Fig. 2**) is seen in these patients with early cirrhosis. These findings are attributed to atrophy of the medial segment of the left hepatic lobe, suggesting that medial segment atrophy may be an initial morphologic change in early cirrhosis.[17]

Hepatic morphologic changes typically seen in advanced cirrhosis include hypertrophy of the caudate lobe and lateral segments of the left lobe, and atrophy of both posterior segments of the right lobe and the medial segment of the left lobe.[17] Other morphologic changes with high specificity for a diagnosis of cirrhosis include the expanded gallbladder fossa sign (**Fig. 3**),[18] which is defined as enlargement of the pericholecystic space (ie, gallbladder fossa), and the right posterior hepatic notch sign (see **Fig. 3**),[19] which is defined as a sharp indentation in the right medial posterior surface of the liver (**Table 1**).

The patterns of hepatic morphologic and signal intensity changes overlap among the different causes of cirrhosis. However, certain imaging features may suggest particular etiological factors, such as enlargement of the lateral segment accompanied by shrinkage of both the right lobe and left medial segment, which reportedly frequently occurs in patients with viral-induced cirrhosis. Conversely, previous study showed

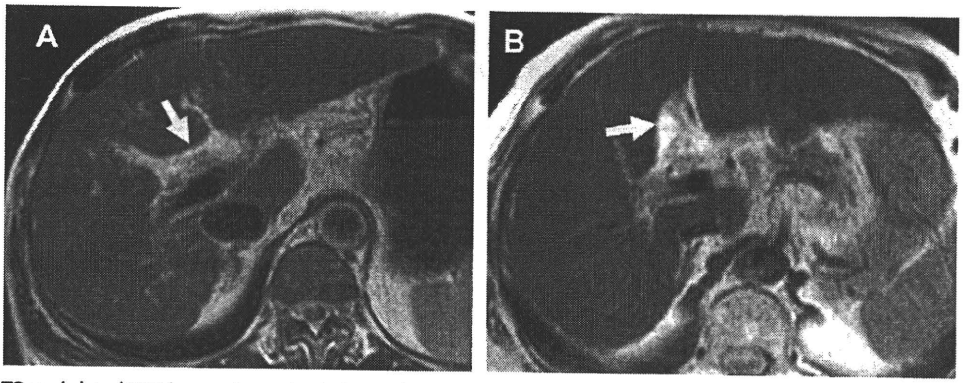

Fig. 2. T2-weighted TSE image in early cirrhosis shows enlargement of the hilar periportal space between the left medial segment and the right portal vein (*A*) (*arrow*) and expansion of the major interlobar fissure (*B*) (*arrow*) between the left medial and lateral segments.

that the mean values of the volume index of the caudate lobe were significantly greater in patients with alcoholic cirrhosis than in patients with viral cirrhosis.[20] Marked caudate lobe enlargement is typically associated with alcoholic cirrhosis.[20]

Primary sclerosing cholangitis (PSC) and primary biliary cirrhosis (PBC) have several distinctive features that may help to differentiate them from other types of cirrhosis (**Table 2**). PSC is reportedly associated with hypertrophy of the caudate lobe and atrophy of the other areas (medial segment, lateral segment, and right hepatic lobe, either individually or in combination) (**Fig. 4**).[21] Previous study showed that these findings were observed in 68% (ie, hypertrophy of the caudate lobe) and 55% (ie, atrophy of the other areas) of patients with PSC, respectively.[21] Other etiologies, such as Budd-Chiari syndrome also demonstrate hypertrophy of the caudate lobe and variable atrophy/hypertrophy of the remaining portions of the liver.[22] In addition, irregular intra- and/or extrahepatic bile duct dilatation and stenosis are also observed. The arterial or delayed phase of contrast-enhanced dynamic MR imaging demonstrates increased enhancement of the hepatic parenchyma surrounding the dilated

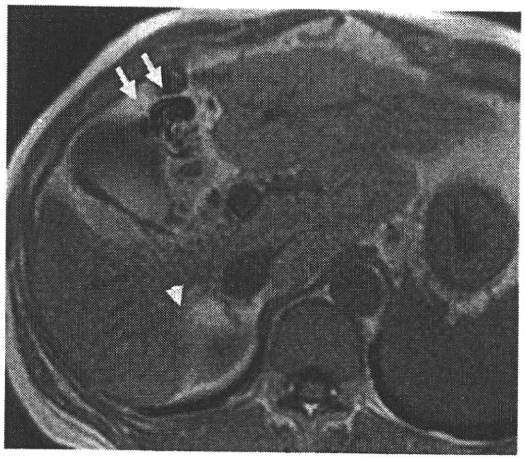

Fig. 3. T1-weighted gradient-echo (GRE) in-phase (TE, 4.7 ms) image in advanced cirrhosis shows enlargement of the pericholecystic space, presenting the expanded gallbladder fossa sign (*arrows*), and sharp indentation in the right medial posterior surface, presenting the right posterior hepatic notch sign (*arrowhead*).

Table 1
Typical morphologic changes of liver cirrhosis

Early Cirrhosis	Advanced Cirrhosis
Enlargement of the hilar periportal space	Hypertrophy of caudate lobe and/or lateral segments
Expansion of the major interlobar fissure	Atrophy of medial and/or posterior segments
	Enlargement of the pericholecystic space (expanded gallbladder fossa sign)
	Hepatic sharp indentation in the posterior surface (right posterior hepatic notch sign)

Data from Refs.[12–16]

Table 2
Distinctive morphologic changes and appearance of PSC and PBC at MR imaging

	Morphologic Changes	Appearance on MR Imaging
PSC	Hypertrophy of caudate lobe Atrophy of medial segment, lateral segment, right hepatic lobe (or all of 3 segments) Dilatation and stenosis of intra- and/or extrahepatic bile duct	Dynamic MR imaging[a] Increased enhancement of local hepatic parenchyma SPIO[b] Decreased enhancement of local hepatic parenchyma Gd-EOB-DTPA[c] Decreased enhancement of local hepatic parenchyma
PBC	Nonspecific	Periportal hyperintensity (hyperintense on T2WI) MR imaging periportal halo sign (hypointense on T1WI and T2WI)

Abbreviations: PBC, primary biliary cirrhosis; PSC, primary sclerosing cholangitis; WI, weighted imaging.
[a] T1-weighted GRE image on arterial- and portal phase after administration of gadolinium-based contrast agents.
[b] T2-weighted GRE image after administration of superparamagnetic iron oxide (SPIO).
[c] T1-weighted GRE image on hepatocyte-selective phase after administration of gadoxetic acid (Gd-EOB-DTPA).
Data from Refs.[17–19]

intrahepatic bile duct (**Fig. 5**), which is considered to represent fibrotic changes and hepatocyte damage.[21] In the authors' experience, the periductal parenchyma in PSC does not show uptake of SPIO, a liver-specific MR contrast agent normally taken up by hepatic Kupffer cells (**Fig. 6**). A reduced uptake of hepatobiliary-specific contrast agents (ie, Gd-EOB-DTPA, discussed later) is also observed (see **Fig. 6**).

MR findings that have been shown to be helpful in the diagnosis of PBC include periportal hyperintensity on T2-weighted images and the periportal halo sign (**Fig. 7**). Periportal hyperintensity on T2-weighted MR images has been attributed to periportal inflammation.[23] One study reported that periportal hyperintensity (see **Fig. 7**) was observed in 100% of patients with PBC with histologic stage I or II disease, 75% of patients with stage III disease, and 33% of patients with stage IV disease.[24] Forty-three percent of patients with PBC are reported to demonstrate the periportal halo sign (see **Fig. 7**), which is depicted as periportal signal hypointensity on T1- and T2-weighted

Fig. 4. T2-weighted fat-saturated TSE image in a patient with primary sclerosing cholangitis (PSC) shows hypertrophy of the caudate lobe (*asterisk*), and atrophy of the medial segment (*arrow*) and right hepatic lobe (*arrowhead*).

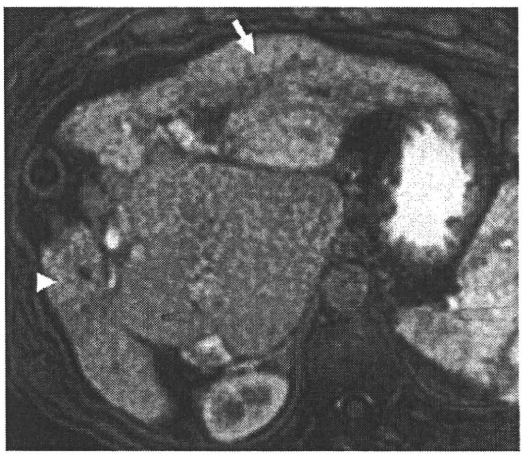

Fig. 5. Arterial-phase contrast-enhanced dynamic MR imaging shows slight increased enhancement of liver parenchyma in the lateral segment (*arrowhead*) and right hepatic lobe (*arrow*), which corresponds to the distribution of intrahepatic bile duct dilatation in comparison with that in caudate lobe. (Same patient as in **Fig. 4.**)

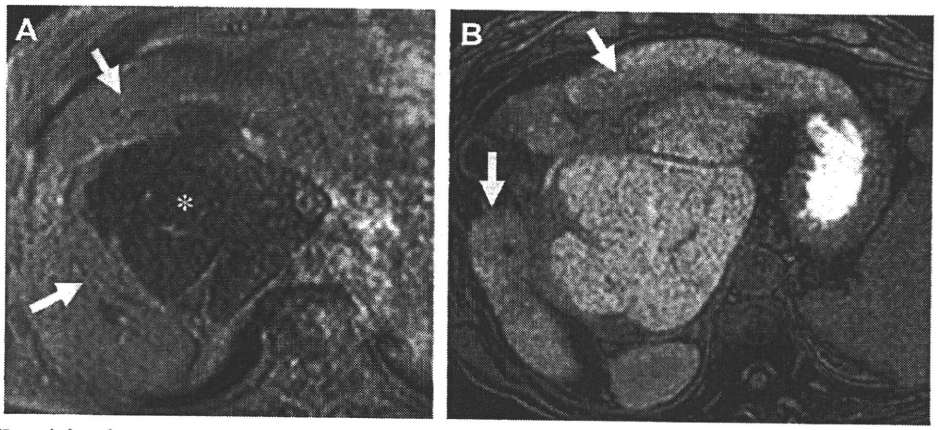

Fig. 6. T2-weighted GRE image (TE, 9.5 ms) within 10 minutes after administration of SPIO (*A*) demonstrates a high-intensity area in which SPIO particles are not taken up, presenting fibrotic change and hepatocyte damage (*arrows*). Conversely, uptake of SPIO particles is observed in the caudate lobe (*asterisk*). T1-weighted fat-saturated 3-dimensional (3D) gradient-echo (GRE) images (TR/TE = 3.6/1.7 ms, flip angle = 15°) in hepatocyte-selective phase (*B*) shows also decrease of uptake of Gd-EOB-DTPA (*arrows*). (Same patient as in **Fig. 4.**)

MR images.[23] It has been suggested that the MR imaging periportal halo sign may represent stellate, periportal, hepatocellular parenchymal extinction encircled by a rosette of large regenerating nodules.[23]

Portal Hypertension

In the cirrhotic liver, progressive hepatic fibrosis leads to increased vascular resistance at the level of the hepatic sinusoids, which results in a reduced portal contribution to liver perfusion.[25] The subsequent development of portal hypertension gives rise to complications such as ascites and the development of collateral vessels at the lower end of the esophagus (**Fig. 8**).[26] Portosystemic shunts also form through reopened paraumbilical veins (see **Fig. 8**) and the left gastric vein, which both normally drain into the portal vein.

The decreased portal venous supply that occurs as a result of liver fibrosis is partially compensated by an increase in arterial blood supply.[27] Such an increase in arterial perfusion may be demonstrated by pronounced liver enhancement in the first seconds after administration of intravenous contrast media in cirrhotic patients. Early patchy enhancement of liver parenchyma on MR imaging is a feature of portal hypertension, and is

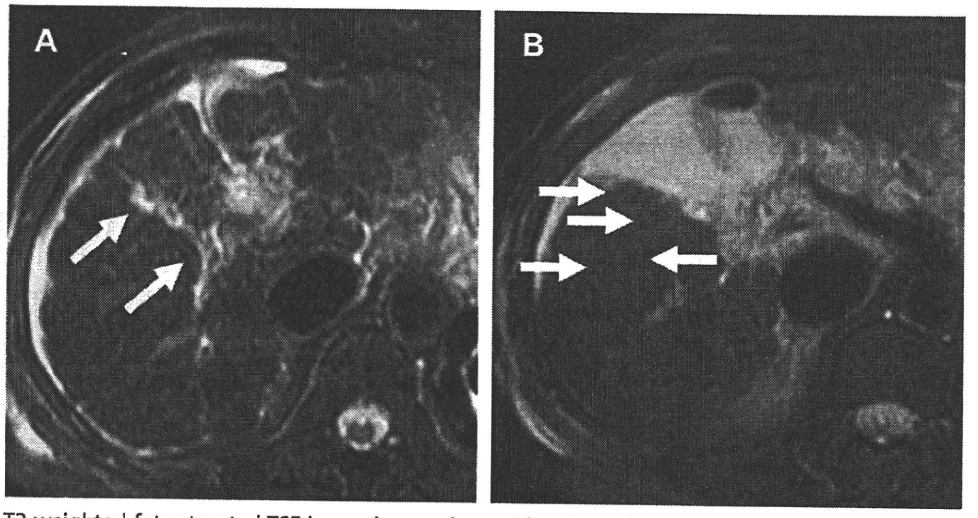

Fig. 7. T2-weighted fat-saturated TSE image in a patient with primary biliary cirrhosis shows periportal hyperintensity (*A*) (*arrows*) around portal tracts and around areas of low-intensity signal (*B*) (*arrows*) encircling the portal veins, presenting the periportal halo sign.

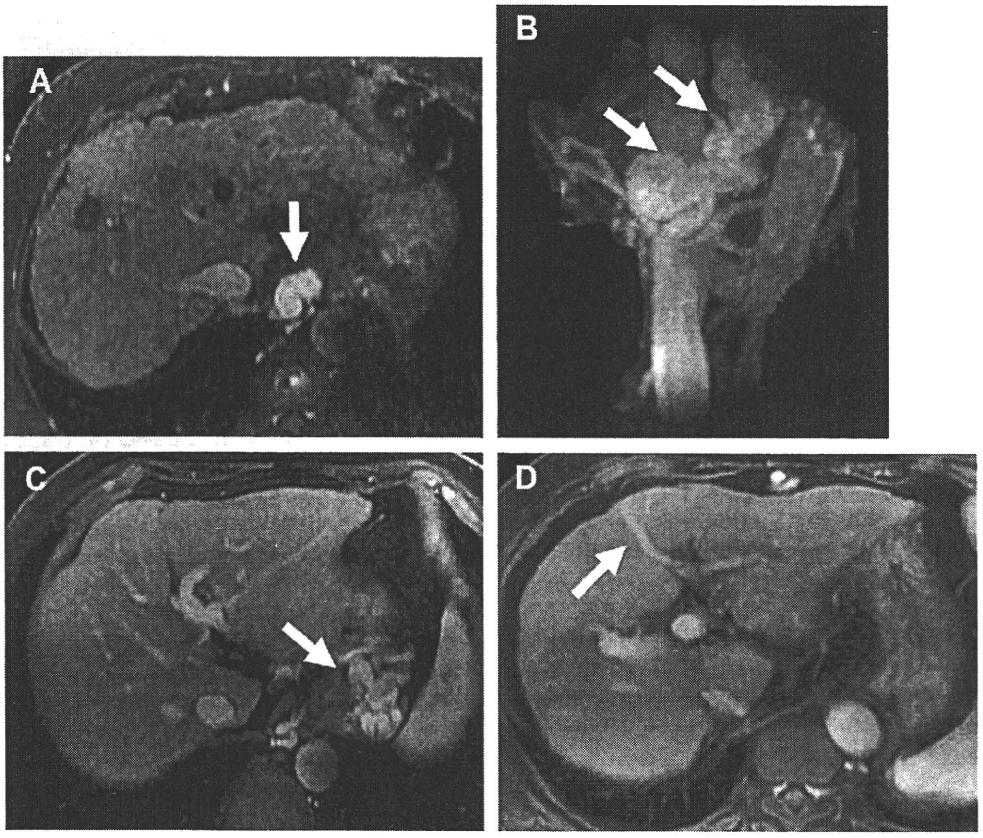

Fig. 8. Axial T1-weighted fat-saturated 3D GRE images (TR/TE = 3.3/1.5 ms, flip angle = 12°) (*A*, *C*, *D*) and maximum-intensity projection image (*B*) in portal phase after administration of Gd-EOB-DTPA at 3-T units shows examples of collateral vessel development in end-stage cirrhosis; dilated and tortuous esophageal varices (*A*, *B*) (*arrows*), gastric varices (*C*) (*arrow*), and recanalized paraumbilical veins (*D*) (*arrow*).

reportedly associated with the presence of numerous infiltrating macrophages, necrosis, tissue collapse, and increased steatosis (**Fig. 9**).[28]

Fibrosis

Pathologic characteristics and MR imaging features of liver fibrosis

Fibrosis is an inherent component of cirrhosis, and has MR imaging characteristics. In viral hepatitis, liver fibrosis begins and manifests as fibrous expansion of the portal triads (**Fig. 10**). Fibrous septa then grow from the expanded portal triad into the surrounding hepatic parenchyma. Subsequently, the fibrous septa lengthen and thicken to eventually form fibrous bridges that link adjacent portal triads and central veins (see **Fig. 10**). As the liver injury continues, the bridges continue to enlarge and coalesce and eventually divide the liver into rounded islands of hepatic parenchyma (regenerative nodules) surrounded by fibrosis tissue (see **Fig. 10**).[29] The pattern of early fibrosis

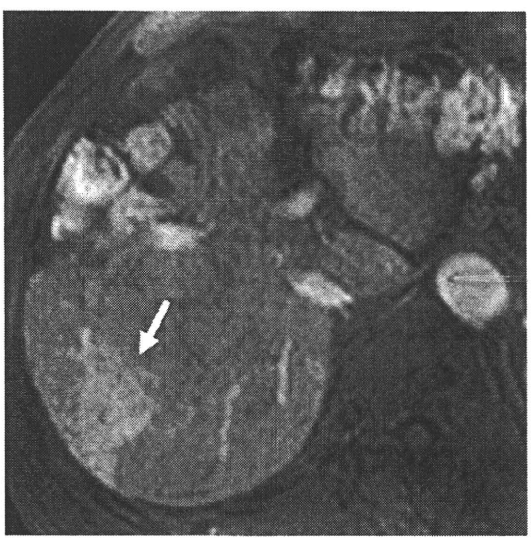

Fig. 9. Arterial-phase contrast-enhanced dynamic MR image shows increased enhancement of liver parenchyma (*arrow*), presenting early patchy enhancement.

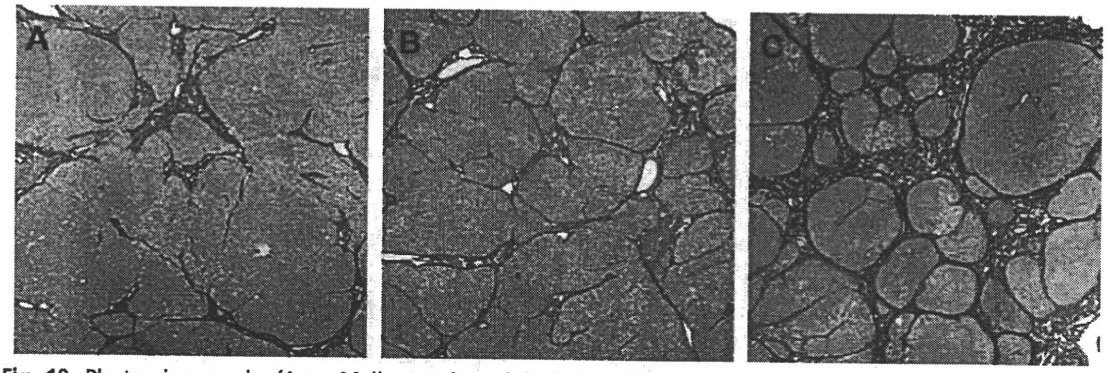

Fig. 10. Photomicrographs (Azan-Mallory stain, original magnification ×20) in a patient with hepatitis C virus infection (HCV) shows chronic hepatitis (*A*), early cirrhosis (*B*), and advanced cirrhosis (*C*). *A* shows moderate fibrosis without lobular distortion, and *B* shows advanced fibrosis having a tendency of lobular distortion. *C* shows multiple regenerative nodules and wider fibrous septa surrounding these nodules. (*Courtesy of* Osamu Nakashima, MD, Department of Pathology, Kurume University School of Medicine, Japan.)

differs in alcoholic hepatitis and nonalcoholic fatty liver disease because early fibrosis first develops adjacent to the central veins rather than in the portal triads, but progressive fibrosis eventually shows the same pathologic findings as cirrhosis caused by viral hepatitis.[29,30]

The current reference examination in the assessment of liver fibrosis is liver biopsy. However, this procedure is invasive with recognized morbidity and mortality, and repeated biopsy for the monitoring of disease progression is accordingly suboptimal. In addition, the accuracy of biopsy remains controversial because of sampling variability caused by the small size of hepatic samples and the heterogeneity of liver fibrosis.[31] These limitations have stimulated the search for noninvasive approaches to the assessment of liver fibrosis.

Conventional MR imaging techniques and fibrosis

The MR imaging appearance of the fibrotic septa and bridges comprises reticulations surrounding regenerative nodules giving rise to the so-called lacelike pattern. The fibrous septa appear hypointense on T1-weighted images and hyperintense on T2-weighted images (**Fig. 11**),[16] which in part is attributed to large water content.[22]

Most gadolinium-based contrast agent formulations freely equilibrate with extracellular volumes, such as liver fibrosis, and thereby improve the visibility of fibrosis on MR imaging.[32] MR images obtained at the equilibrium and delayed phase after gadolinium administration show fibrotic septa and bridges as linear and reticulation enhancement patterns.[28] These findings are more prominent in the periphery of the liver.

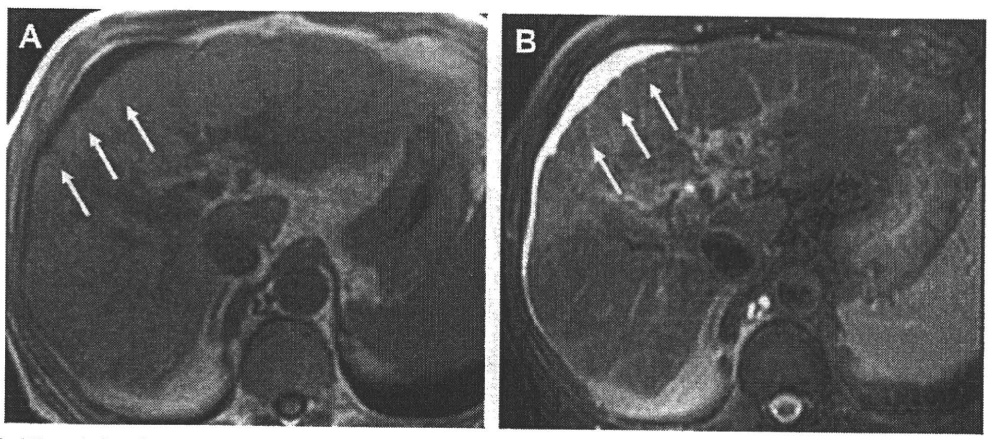

Fig. 11. T1-weighted GRE in-phase (TE, 4.7 ms) image and T2-weighted fat-saturated TSE image shows fibrotic septa and bridges as reticulations. The reticulations (*arrows*) are observed as hypointense on T1-weighted images (*A*) and as hyperintense on T2-weighted images (*B*).

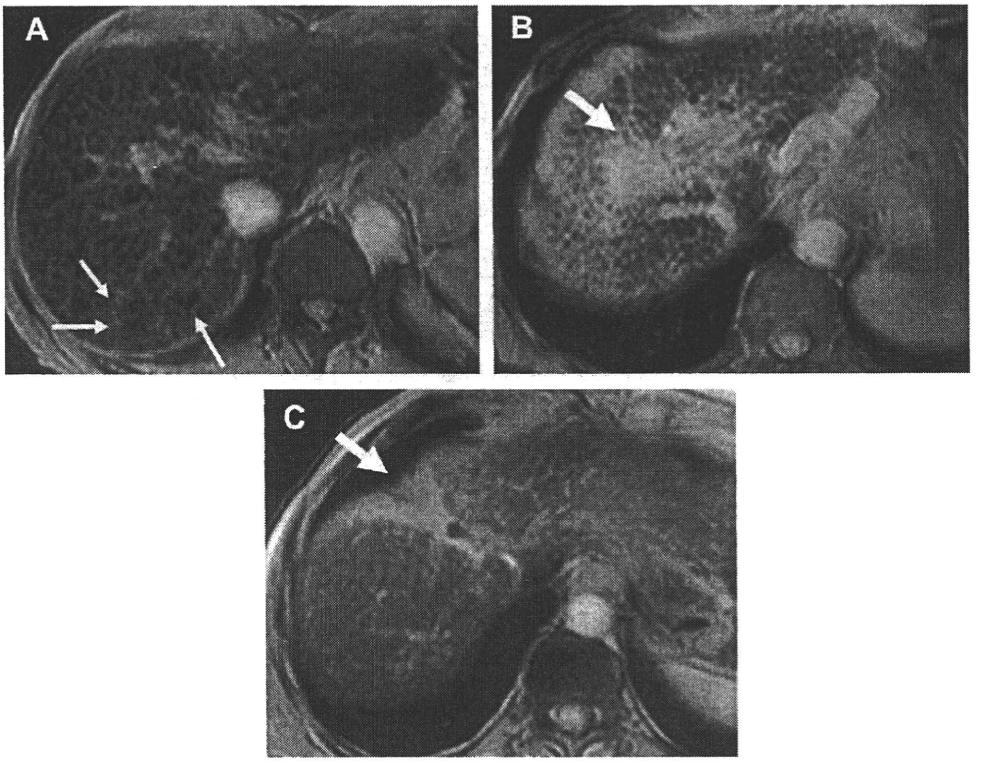

Fig. 12. T2-weighted GRE image (TE, 9.5 ms) after administration of SPIO distinctly demonstrates high-intensity reticulations (*A*) (*arrows*) and confluent fibrosis (*B* = wedge shape, *C* = geographic shape) (*arrow*), which do not take up SPIO particles in cirrhotic liver with HCV.

In end-stage liver cirrhosis, focal confluent fibrosis, which typically has a wedge shape or geographic shape with straight or concave borders, is occasionally observed in the subcapsular region.[22,28] The signal intensity and enhancement features of confluent fibrosis following administration of extracellular contrast agents are similar to those of fibrotic septa and bridges.

Liver-specific contrast agents and fibrosis

SPIO-enhanced MR imaging has been shown to be helpful in the detection of macroscopic fibrous bands and diffuse liver fibrosis. On T2-weighted turbo spin-echo and T2-weighted GRE images after administration of SPIO, the areas of fibrosis within the liver, which have reduced Kupffer cell density, accumulate less iron oxide

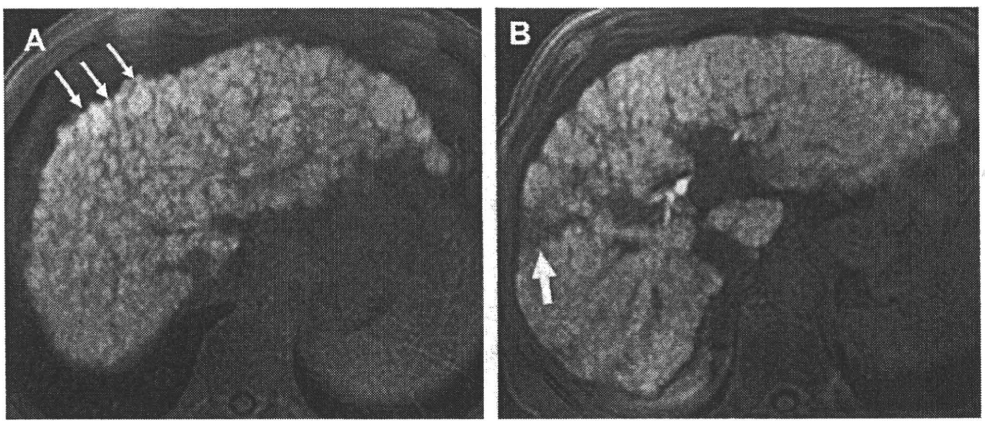

Fig. 13. T1-weighted fat-saturated 3D GRE image (TR/TE = 3.6/1.7 ms, flip angle = 15°) after administration of Gd-EOB-DTPA at hepatocyte-selective phases also clearly demonstrates fibrotic reticulations (*A*) and confluent fibrosis (*B* = wedge shape) (*arrows*).

Table 3
Macroscopic architectures and typical appearance of liver fibrosis at MR imaging

Macroscopic Findings	MR Imaging Form	Signal Intensity	Dynamic MR Imaging[a]	SPIO[b]	Gd-EOB-DTPA[c]
Fibrotic septa and bridge	Reticulation (lacelike pattern)	Hypointense (T1WI)	Increased enhancement	Hyperintense[d]	Hypointense[d]
Confluent fibrosis	Wedge shape or geographic shape	Hyperintense (T2WI)			

Abbreviations: Gd-EOB-DTPA, gadoxetic acid; SPIO, superparamagnetic iron oxide.
[a] T1-weighted GRE image on delayed phase after administration of gadolinium-based contrast agents.
[b] T2-weighted GRE image after administration of SPIO.
[c] T1-weighted GRE image on hepatocyte-selective phase after administration of Gd-EOB-DTPA.
[d] Appearance is described in comparison with the surrounding hepatic parenchyma.
Data from Refs.[13,23,24,26–28,30,31]

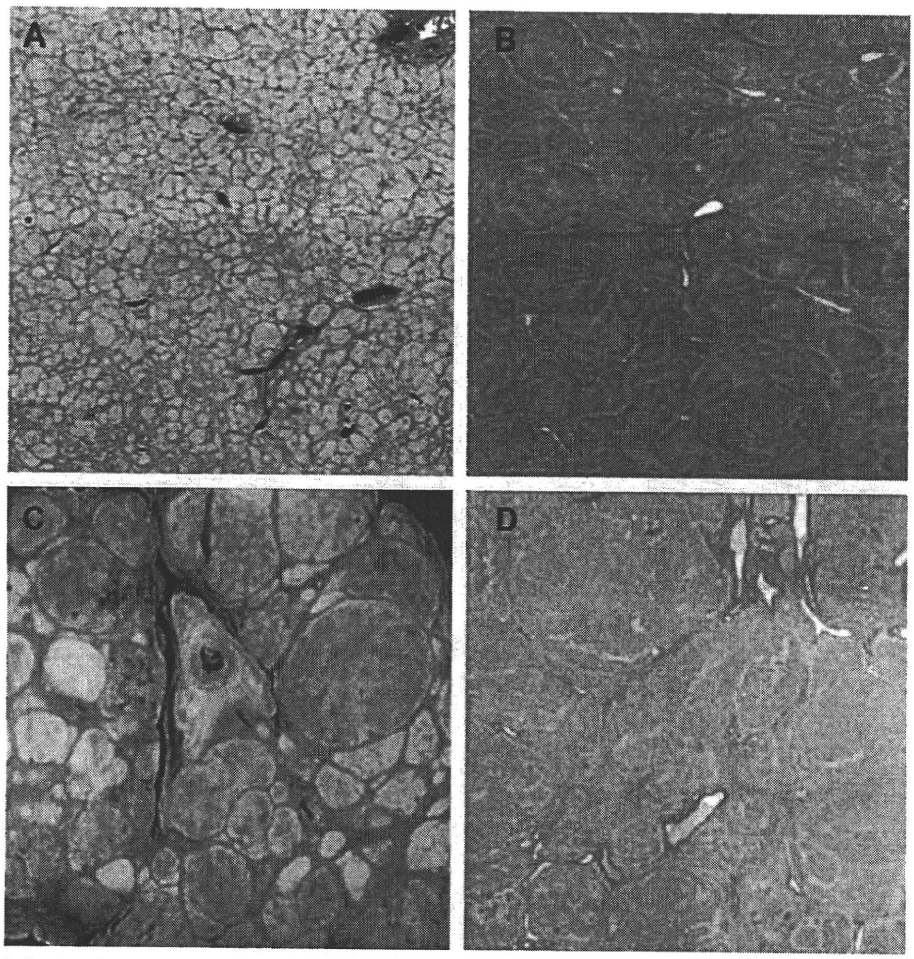

Fig. 14. Cirrhosis of micro- (*A*, *B*) and macronodular type (*C*, *D*). Gross appearance (*A*) and photomicrographs (Azan-Mallory stain, original magnification ×20) (*B*) show regenerative nodules (2–3 mm in size) with irregular shape in a case of cirrhotic liver with HCV. Gross appearance (*C*) and photomicrographs (Azan-Mallory stain, original magnification ×20) (*D*) show regenerative nodules (1–2 cm in size) with regular shape in a case of cirrhotic liver with HBV. (*Courtesy of* Osamu Nakashima, MD, Department of Pathology, Kurume University School of Medicine, Japan.)

and appear as hyperintense reticulations or areas (ie, confluent fibrosis)[33] compared with the surrounding hepatic parenchyma (**Fig. 12**). A recent study has shown the usefulness of double-contrast–enhanced MR imaging (sequential administration of SPIO and a gadolinium-based contrast agent) in the detection of liver fibrosis architecture. The investigators noted that the combination of these contrast agents was synergistic, and demonstrated liver fibrosis with greater clarity than could be achieved with either agent alone.[34]

Hepatobiliary-specific contrast agents such as mangafodipir trisodium (Mn-DPDP), gadobenate dimeglumine (Gd-BOPTA), and Gd-EOB-DTPA are taken up by functioning hepatocytes and excreted in the bile. The paramagnetic properties of these agents cause shortening of the longitudinal relaxation time (T1) of the liver and biliary tree. In visual analysis of images enhanced by Mn-DPDP, lower or heterogeneous enhancement areas are observed in cirrhotic liver, and it is considered that these areas contain the fibrous zone, indicating reticulation, confluent, and hepatocyte necrosis.[35,36] In the authors' experience, images enhanced by Gd-EOB-DTPA frequently show similar findings in cirrhotic liver, and this agent may also distinctly demonstrate liver fibrosis, such as fibrous septa, bridges (**Fig. 13**), and confluent fibrosis (see **Fig. 13**) (**Table 3**).

Emerging functional MR imaging techniques for fibrosis

Recently, several novel techniques for the assessment of liver fibrosis have been proposed, including MR elastography, diffusion-weighted MR imaging, and MR spectroscopy. MR elastography is a phase contrast-based MR imaging technique for direct visualization and quantitative measurement of propagating mechanical shear waves in biologic tissue.[37] Recent studies in patients with a spectrum of liver disease types have shown that liver stiffness as measured with MR elastography increases as the stage of fibrosis advances. The difference in stiffness between patients with early stages of fibrosis (F0 vs F1 vs F2) are small, with overlap between groups, but those between groups at higher stages (F2 vs F3 vs F4) are large, with little overlap.[38] Evaluation of the reproducibility and validity of MR

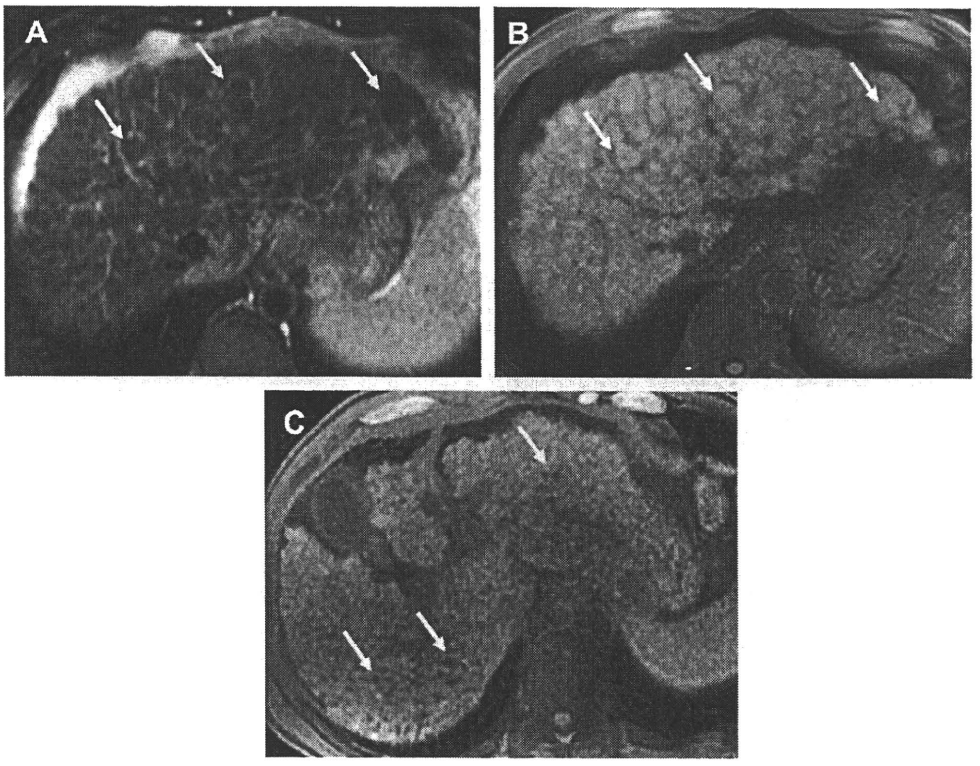

Fig. 15. Innumerable regenerative nodules have varying signal intensity, appearing isointense to hypointense on a T2-weighted fat-saturated TSE image (*A*) (*arrows*) and isointense to hyperintense on a T1-weighted fat-saturated 3D GRE image (TR/TE = 3.6/1.7 ms, flip angle = 15°) (*B*) (*arrows*). Hemosiderin deposition is common in regenerative nodules (siderotic nodules), producing such specific imaging features as hypointensity on T1-weighted fat-saturated 3D GRE image (*C*) (*arrows*).

Table 4
Characteristics and typical appearance of cirrhotic nodules at MR imaging

		Signal Intensity		Dynamic MR Imaging[a]	Kupffer Cell Density	SPIO[b]	Hepatocellular Function	Gd-EOB-DTPA[c]
		T1WI	T2WI					
RNs		Iso–Hyper (siderotic nodules; T1/T2WI, hypo)	Iso–Hypo	Iso–Hyper	Similar[d]	Iso[d]	Similar[d]	Iso[d]
DNs	Low grade	Hypo–Hyper	Hypo	Iso–Hyper	Various[d]	Hypo–Hyper[d]	Various[d]	Hypo–Hyper[d]
	High grade		Hypo–Slightly hyper					

Abbreviations: DNs, dysplastic nodules; Gd-EOB-DTPA, gadoxetic acid; Hypo, hypointense; Hyper, hyperintense; Iso, isointense; RNs, regenerative nodules; SPIO, superparamagnetic iron oxide.

[a] T1-weighted GRE image on delayed phase after administration of gadolinium-based contrast agents.
[b] T2-weighted GRE image after administration of SPIO.
[c] T1-weighted GRE image on hepatocyte-selective phase after administration of Gd-EOB-DTPA.
[d] Appearance is described in comparison with the surrounding hepatic parenchyma.
Data from Refs.[47–55,59–61]

elastography in an independent population of 35 healthy individuals and 48 patients with varying degrees of chronic liver disease showed a sensitivity of 86% and specificity of 85% for the detection of stages 2 to 4 fibrosis compared with liver histology from biopsy. A high negative predictive value (97%) for excluding the presence of fibrosis was also noted, suggesting that MR elastography might have a role in improving the ability to risk-stratify patients for liver biopsy to exclude occult advanced fibrosis.[39] MR elastography therefore appears to shows promise for the noninvasive staging of liver fibrosis, particularly in patients with advanced fibrosis.

Diffusion-weighted magnetic resonance imaging is a technique that assesses the freedom of diffusion of water protons within tissue by applying motion-sensitizing gradients that cause diffusing protons to lose signal. Recent advances in MR imaging technology have facilitated the performance of diffusion-weighted MR imaging of the liver, and it has also been used to detect liver fibrosis. Prior studies have reported that apparent diffusion coefficient (ADC) values acquired from b values of 500 (seconds/mm^2) and greater correlated significantly with liver fibrosis stage, and that ADC values with a combination of b value of 0 and 1000 (seconds/mm^2) showed the highest correlation ($r = -0.654$, $P<.001$).[40] On the other hand, several studies noted that there was no significant correlation between fibrosis stage and the ADC value using low b values (b values, 50 to 400 seconds/mm^2), because diffusion-weighted imaging with a low b value was influenced by perfusion contamination.[40,41] Luciani and colleagues,[42] reported that ADC calculated from low b values was significantly reduced in cirrhosis. Thus, the fast component diffusion-weighted MR imaging

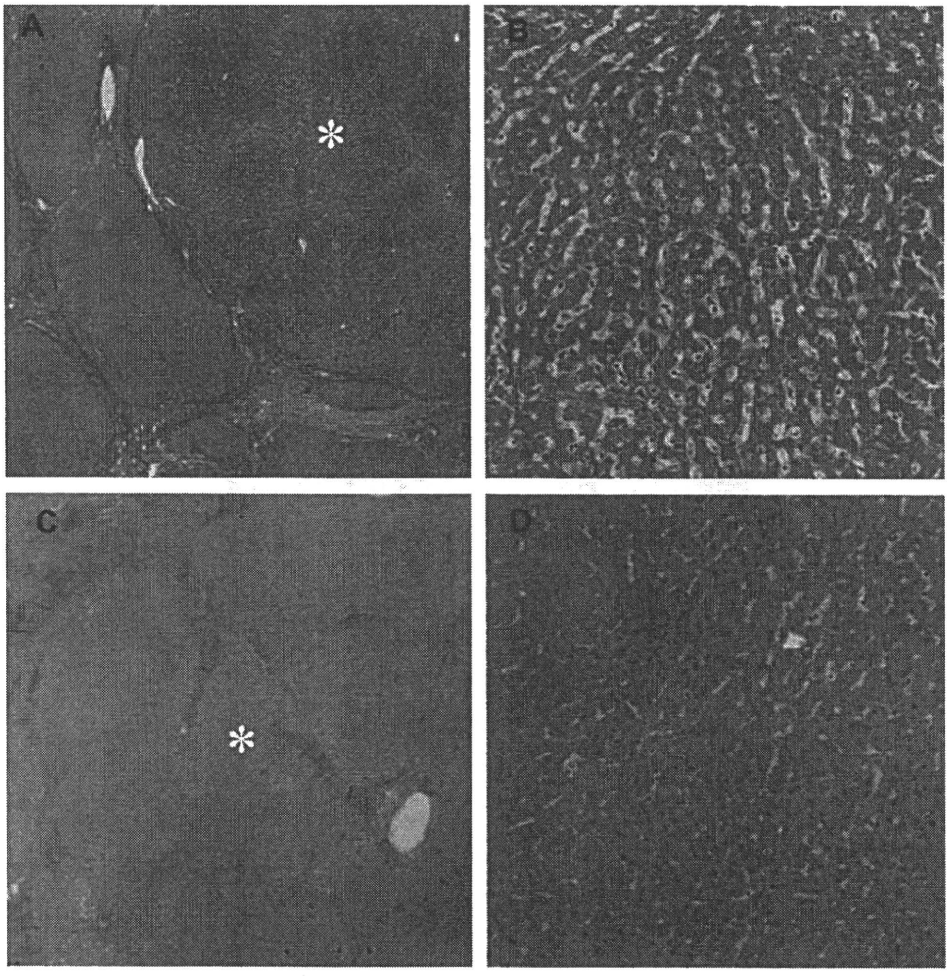

Fig. 16. Photomicrographs (Azan-Mallory stain, original magnification ×20 and ×100) in a patient with HCV shows low-grade dysplastic nodule (*asterisk*) (*A*, *B*) and high-grade dysplastic nodule (*asterisk*) (*C*, *D*). (*Courtesy of* Osamu Nakashima, MD, Department of Pathology, Kurume University School of Medicine, Japan.)

obtained with low b values may provide information related to microperfusion changes in diffuse liver disease whereas the slow component diffusion-weighted MR imaging obtained with high b values has been suggested to reflect a decrease in water proton diffusion.[43] The principles of diffusion-weighted MR imaging is discussed further in this presentation on functional MR imaging techniques.

In vivo MR spectroscopy (MRS) is most commonly used to assess signals from hydrogen (^{1}H) and phosphorus (^{31}P). Although ^{1}H-based MRS allows for the quantification of certain metabolites and lipids, ^{31}P-based MRS provides insights on processes, including cell turnover and energy state, based on the substantial ^{31}P concentrations within hepatocytes.[44] Previous studies have suggested MRS may be useful in detecting hepatic fibrosis.[45,46] An increased levels of hepatic phosphomonoesters (PME) have been reported in patients with established cirrhosis,[45,46] and an increasing PME to phosphodiester (PDE) ratio has been reported to correlate with worsening necroinflammatory and fibrosis scores on liver histology.[47] It has also been suggested that a PME and PDE ratio 0.2 or less is correlated with mild hepatitis and 0.3 or greater is correlated with cirrhosis in a study involving patients with chronic hepatitis C.[48] Despite some preliminary promising data, ^{31}P-based MRS is not widely used due to specific technical requirements. The role of MRS in the detection of liver inflammation and fibrosis requires further investigation.

CIRRHOSIS-ASSOCIATED HEPATOCELLULAR NODULES

Regenerative Nodules

Regenerative nodules form in response to necrosis, altered circulation, or other stimuli,[49] and may progress along a well-described carcinogenetic pathway to become dysplastic nodules or hepatocellular carcinomas.[50] These nodules are present in all cirrhotic livers and are surrounded by fibrous septa (see **Fig. 10**).[16] The nodules may be monoacinar or multiacinar, depending on

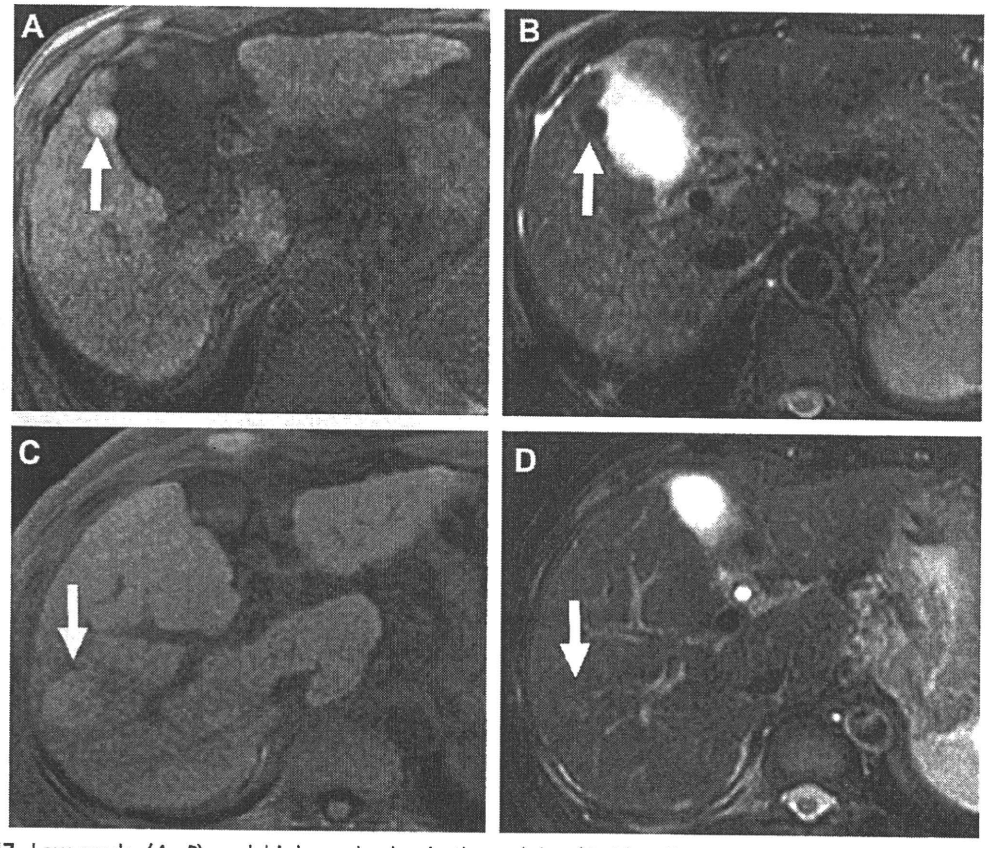

Fig. 17. Low-grade (*A*, *B*) and high-grade dysplastic nodules (*C*, *D*). All nodules were hyperintense on T1-weighted fat-saturated 3D GRE images (TR/TE = 3.6/1.7 ms, flip angle = 15°) (*A*, *C*) (*arrows*). In T2-weighted fat-saturated TSE images, in contrast, a low-grade dysplastic nodule is observed as hypointense (*B*) (*arrow*), whereas a high-grade nodule is observed as slightly hyperintense (*D*) (*arrow*).

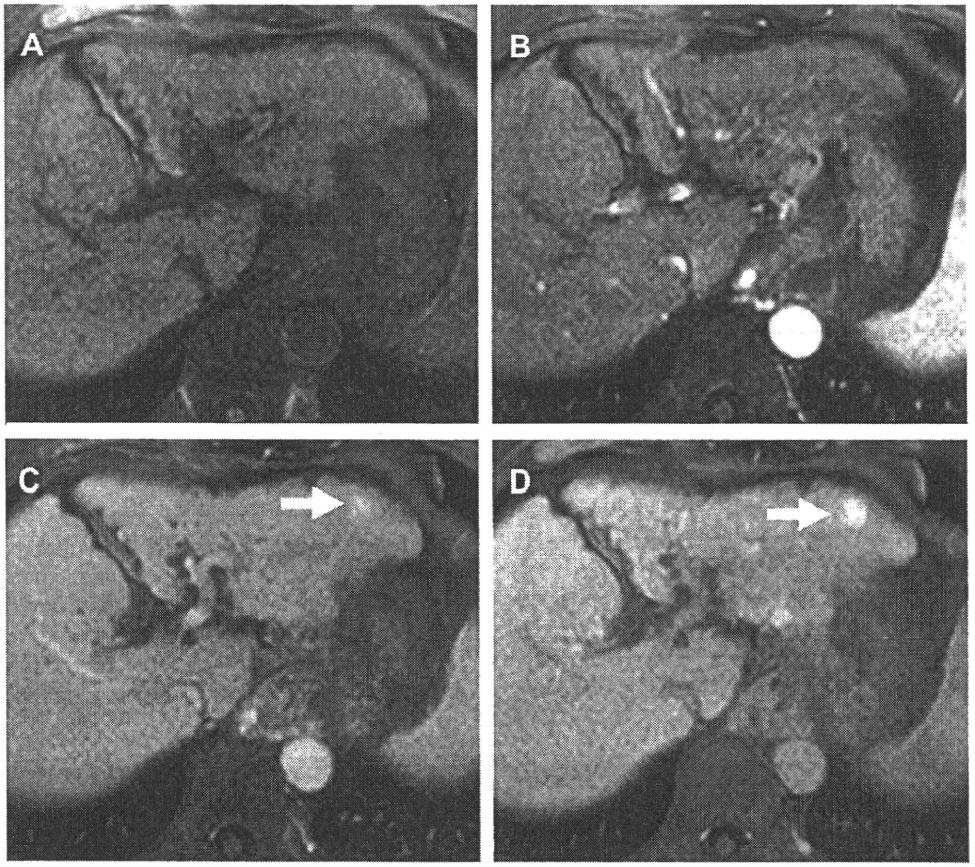

Fig. 18. Dynamic enhancement patterns of a high-grade dysplastic nodule in axial T1-weighted fat-saturated 3D GRE images (TR/TE = 3.6/1.7 ms, flip angle = 15°), presenting before (*A*) and in the arterial phase (30 s) (*B*), portal phase (90 s), and (*C*) equilibrium phase (4 min), and (*D*) after intravenous injection of Gd-EOB-DTPA. Portal and equilibrium phases (*arrow*) show increased enhancement of high-grade dysplastic nodule.

whether they contain one or more terminal portal tracts, and can also be classified by size as of the micronodular (≤3 mm) (**Fig. 14**), macronodular (>3 mm) (see **Fig. 14**), or mixed type (features of both micro- and macronodular types).[51]

MR imaging demonstrates regenerative nodules with greater sensitivity than any other imaging modality. These nodules usually appear isointense to hypointense (**Fig. 15**) on T2-weighted images relative to the surrounding inflammatory fibrous septa, and isointense to hyperintense (see **Fig. 15**) relative to background liver parenchyma on T1-weighted images.[52] The accumulation of iron within regenerative nodules (siderotic nodules) may cause hypointensity on both T1- and T2-weighted images (see **Fig. 15**) owing to susceptibility effects.[53] With regard to blood supply on dynamic imaging, regenerative nodules are usually enhanced to the same or greater degree than the background liver in the portal venous phase,[54] owing to the large contribution from the portal vein, with minimal contribution from the hepatic artery (**Table 4**).[55]

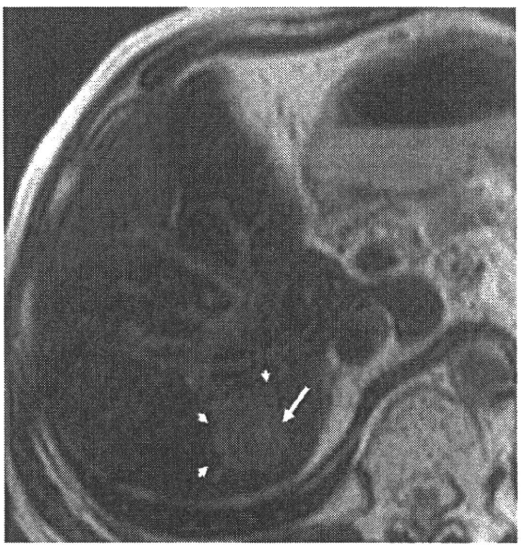

Fig. 19. T2-weighted TSE image shows an iso- to slightly high-signal–intensity nodule (*arrowheads*) with a focus of higher signal intensity (*arrow*) within the nodule. This higher signal intensity focus within the nodule shows the presence of HCC.

Dysplastic Nodules

Dysplastic nodules are considered an intermediate, premalignant step along the hepatocarcinogenesis process, and can also be classified by the degree of dysplasia as low- or high-grade.[56]

Low-grade dysplastic nodules are sometimes vaguely nodular but are often distinct from the surrounding cirrhotic liver because of the presence of peripheral fibrous scar.[56] This nodule is not a true capsule, but rather condensation of scarring as is seen around all cirrhotic nodules. Low-grade dysplastic nodules show mild increase in cell density with a uniform pattern, and without cytologic atypia.[56] Architectural changes beyond clearly regenerative features are not present; these lesions do not contain pseudoglands or markedly thickened trabeculae (**Fig. 16**).[56] High-grade dysplastic nodules may also be distinctly or vaguely nodular in the background of cirrhosis, although they also lack a true capsule, similar to low-grade dysplastic nodules; however, they are more likely to show a vaguely nodular pattern than low-grade dysplastic nodules.[56] A high-grade dysplastic nodule is defined as having architectural and/or cytologic atypia, but the atypia is insufficient for a diagnosis of HCC.[56] These lesions most often show increased cell density, sometimes more than 2 times higher than the surrounding nontumoral liver, often with an irregular trabecular pattern (see **Fig. 16**).[56] On MR imaging, dysplastic nodules have variable

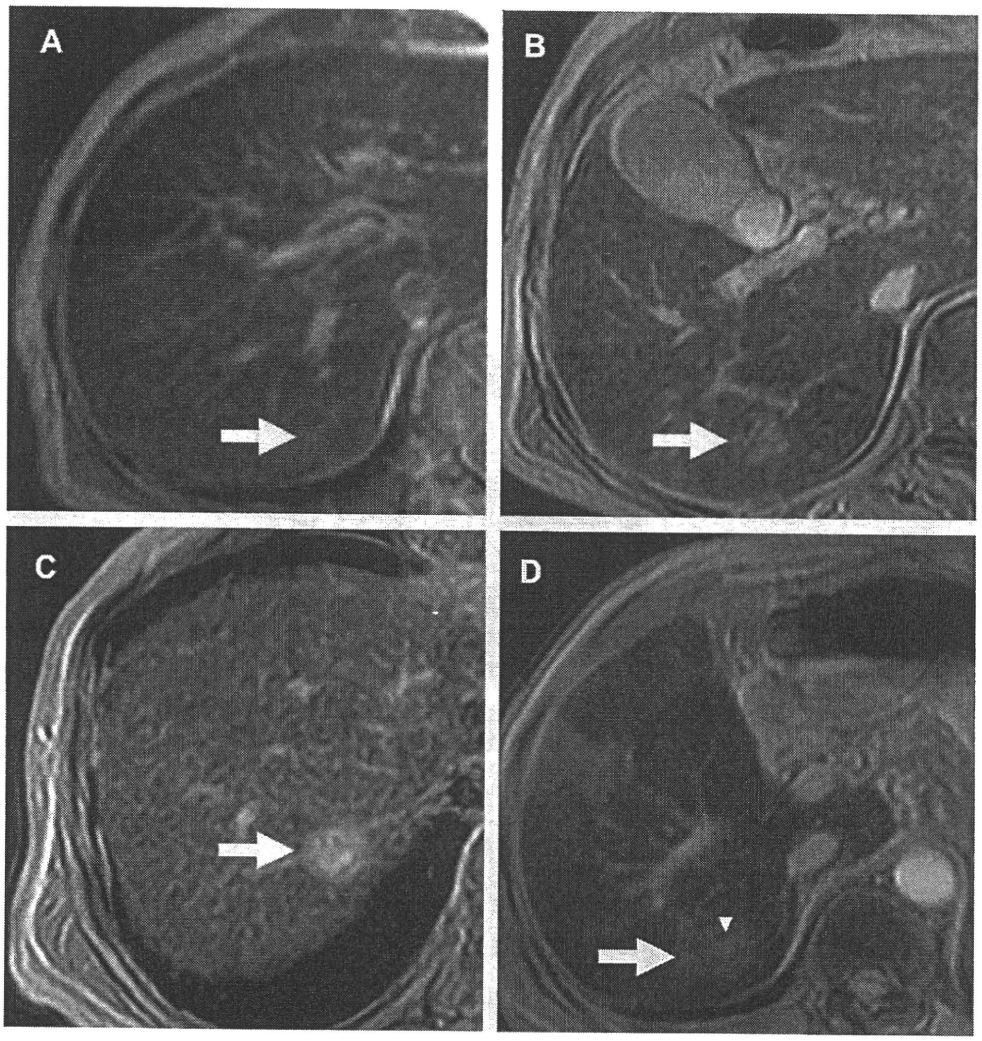

Fig. 20. T2-weighted GRE images (TE, 9.5 ms) after administration of SPIO in well-differentiated hepatocellular carcinoma (HCC) shows various signal intensities depending on Kupffer cell function within the nodule (*A–D*) (*arrow*). A dysplastic nodule with a central focus of HCC is observed as "a nodule within a nodule" (*D*) (*arrowhead*).

appearances, and their signal intensity characteristics overlap with those of regenerative nodules and well-differentiated HCC. On T2-weighted images, most dysplastic nodules are usually hypointense, and only rarely hyperintense (**Fig. 17**) It has been suggested that high-grade dysplastic nodules tend to have slightly higher signal intensity on T2-weighted images (see **Fig. 17**)[57]; however, the distinction from HCC and a high-grade dysplastic nodule may be difficult even on pathology. On T1-weighted images dysplastic nodules characteristically demonstrate high signal intensity, which may be related to deposition of copper, Fe^{3+}, or glycogen, or a high protein or lipid content (see **Fig. 17**).[58,59] However, the appearance on T1-weighted images cannot be used to distinguish low- and high-grade dysplastic nodules because both display variable (low, iso-, or high) signal intensity.[57]

With regard to blood supply, dysplastic nodules are typically hypovascular lesions with predominantly portal venous blood supply, although increased arterial flow is seen in a small minority of cases (**Fig. 18**) (see **Table 4**).[60] The signal intensity characteristics of some high-grade dysplastic nodules that receive increasing supply from the hepatic artery may overlap with those of HCC nodules during the process of hepatocarcinogenesis.[61] The hepatocarcinogenesis theory has been supported by the description of a dysplastic nodule with a central focus of HCC on T2-weighted images as "a nodule within a nodule."[62] The classic MR appearance is a focus of high signal intensity within a low-signal–intensity nodule on T2-weighted images (**Fig. 19**). This focus of HCC may also be enhanced in the arterial phase.[63] Despite the possibility of HCC developing within dysplastic nodules, the development of this tumor may not be a linear process because HCC is recognized to occur in patients with chronic HBV but without cirrhosis.

Liver-Specific MR Contrast Agents (SPIO, Gd-EOB-DTPA) for Liver Nodules

Because the density of Kupffer cells within regenerative nodules is similar to that in the surrounding nonneoplastic hepatic parenchyma, these nodules take up SPIO through Kupffer cell phagocytosis. On T2-weighted GRE and T2-weighted spin-echo sequences after administration of SPIO, regenerative nodules show the same signal intensity as that of surrounding hepatic parenchyma. In contrast, because Kupffer cell density within

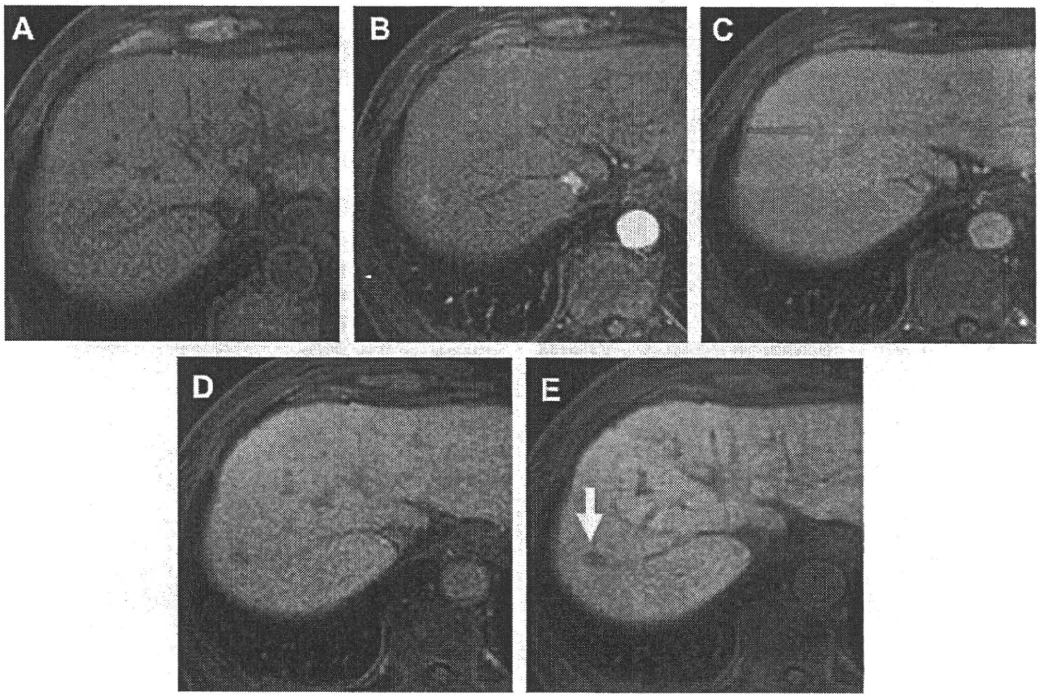

Fig. 21. Dynamic enhancement patterns of well-differentiated HCC in axial 3D fat-saturated T1-weighted GRE images (TR/TE = 3.6/1.7 ms, flip angle = 15°), presenting before (*A*) and in the arterial phase (*B*), portal phase (*C*), equilibrium phase (*D*), and hepatocyte-selective phase (*E*) after intravenous injection of Gd-EOB-DTPA. Well-differentiated HCC is commonly observed as hypointense in the hepatocyte-selective phase (*arrow*).